RESEARCH ARTICLE

Molecular Modeling of Metalloreductase STEAP2 Protein and Docking Interaction Studies: An *In Silico* Study

M. Vamshi Venkat, Shravan Kumar Gunda*, Sharada Durgam, Mahmood Shaik

Division of Bioinformatics, Prof. G. Ram Reddy Centre for Distance Education, Osmania University, Hyderabad, Telangana, India

ABSTRACT

This gene is an individual from the STEAP family and encodes a multipass film protein that confines to the Golgi complex, the plasma layer, and the vesicular cylindrical structures in the cytosol. A very comparative protein in mouse has both ferrireductase and cupric reductase action and invigorates the cell take-up of both iron and copper *in vitro*. Expanded transcriptional articulation of the human quality is related with prostate malignant growth movement. Substitute transcriptional graft variations, encoding distinctive isoforms, have been described. Therefore, in the present study, we generated a precise three-dimensional (3D) model of metalloreductase STEAP2 protein using MODELLER 9.21 and validated its structure using PROCHECK software. Modeled protein contains more than 94.5% of amino acids in core region. We interpreted the action of natural compounds docking against the modeled metalloreductase STEAP2 protein. Three compounds (ginkgetin, medicagenin, and erybraedin A) showed lower binding affinity values toward metalloreductase STEAP2 protein compared to mitoxantrone, abiraterone acetate, apalutamide, enzalutamide, and flutamide. Ginkgetin exhibited the lowest binding energy of −9.10 kcal/mol with interacting Trp212 and Thr210. All the 17 compounds showed excellent binding energies than standard drugs for the modeled metalloreductase STEAP2 protein. These computational studies can be helpful to discover novel drug candidates.

Keywords: Docking studies, flavonoids, homology modeling, metalloreductase STEAP2

INTRODUCTION

Prostate malignant growth is an illness and is asymptomatic in its beginning periods that influence men extending from 45 to 80 years old.[1] Even it is the most prevalent in men beyond 75 years old and as numerous men follow an apathetic course without the progress of metastatic infection and the rate of prostate cancer has expanded worldwide as of late. While prostate disease is the most widely recognized malignancy and second driving reason for death in men. The proof based on the conclusion and treatment of prostate malignant growth is continuously fluctuating. Prostate-specific antigen (PSA) testing to identify prostate malignant growth at a beginning time has brought about expanding quantities of men being determined to have little measured tumor volumes upgrading the therapeutic treatment of these tumors.[2] PSA levels are utilized close by clinical stage and prostate biopsy Gleason score to decide the danger of repeat and additionally movement after starting finding of non-metastatic illness.[3] Metastasis represents the fundamental driver of disease mortality also, is a procedure, whereby the essential site tumor cells gain the capacity to spread to an auxiliary site.[4]

In eukaryotes, iron and copper metabolism are complicatedly interrelated.[5,6] Iron and copper are basic for all life forms, accepting basic jobs as cofactors in numerous compounds. STEAP2,

_____

*Corresponding Author:
Shravan Kumar Gunda,
E-mail: gunda14@gmail.com

STEAP3, and STEAP4 are ferrireductases as well as likewise cupric reductases that invigorate cell take-up of both iron and copper *in vitro* the instances of explanation in tissues basic in iron and copper homeostasis and the subcellular confinement of these proteins recommends that they might be imperative metalloreductases *in vivo*.[7] In spite of the way, this may be required rather to improved screening and identifcation methods.[7]

Matrix metalloproteinases (MMPs) can corrupt an assortment of cell attachment particles bringing about the regulation of cell–cell and cell-extracellular matrix interactions. Moreover, ongoing proof has exhibited that the protein six transmembrane epithelial antigen of the prostate (STEAP2) expands Extracellular signal-regulated kinase (ERK) flagging, a particle whose downstream effectors are MMPs it likewise goes about as a ferrireductase and cupric reductase which animates the take-up of iron and copper into the cell. STEAP2 has been appeared to influence prostate malignant growth cell development, as its down control results in the up direction of some cell cycle inhibitors and furthermore influences cell multiplication, when down managed, apoptosis levels are expanded. One of the prostate-specific genes upregulated in prostate cancer is STAMP1 (also known as STEAP2). The role of STAMP1 in prostate cancer cells, or its biological expression profile at the protein level, is not known.[8]

STAMP1 articulation is androgen free, however, for the most part happens in androgen receptor (AR) positive cells. STAMP1 articulation is fundamentally expanded in prostate malignancy contrasted and typical prostate.[9] STEAP2 expression is widely elevated in various different cancers. STEAP2 is currently considered as a critical symptomatic creator and remedial target. Due to the overexpression of STEAP2, specifically in intrusive prostate cancer, we guessed that STEAP2 may play fundamental robotic job in movement to cutting edge illness.

METHODOLOGY

Sequence alignment and structure prediction

The amino acid sequence of metalloreductase STEAP2 protein (Accession number Q8NFT2),[10]

from the species *Homo sapiens* was retrieved from the UniProtKB database (http://www.uniprot.org/). Template was selected by aligning query sequence using protein BLAST.[11] After running protein BLAST, the template crystal structure of Chain C, metalloreductase STEAP2 protein (protein databank [PDB] ID: 6HCY_C) with 47.50% similarity having a resolution of 3.1 Å was selected on the basis of identity, similarity, gap penalty, and E-value. The three-dimensional structure was generated using MODELLER 9.21. The respective template was downloaded from PDB.[12] The predicted model was further validated using PROCHECK[13] for Ramachandran plot. Both (query and template) proteins were superimposed and calculated the root-mean-square deviation (RMSD) to access the accuracy and reliability of the generated model.

MODELLER 9.21 was then used to gain satisfactory models. MODELLER is an automated approach to homology modeling by satisfaction of spatial restraints. Sequence alignment performed for both query and template sequences with offline and online tools such as ClustalX and Clustalw2[14] which are shown in Figure 1. MODELLER 9.21 tool[15] was used to construct the model for query metalloreductase STEAP2. After initial alignment, 20 models were generated. The best model is selected on the basis of lower MODELLER objective function value. The stereochemical quality of the given models is then evaluated using specific software like PROCHECK and the model can be used for further structural or functional study. Ramachandran plot explains the residues by residue listing facilitates the in-depth calculation of Psi/Phi angles and the backbone conformation of the models.

Docking methodology

Identification of active site pockets

The active site prediction was carried out using Tripo's Sybyl6.7. It showed three active site pockets. The amino acids which are present in pocket one are Asn256, Pro260, Ile261, Ala263, Ile264, Leu267, Val270, Tyr271, Arg302, Lys303, Gly306, Leu307, Ser309, His316, Gly364, Ser367, Leu368, Leu371, Leu374, Ile394, Leu398, Gly399,

```
sp|Q8NFT2|STEA2_HUMAN    MESISMMGSPKSLSETFLPNGINGIKDARKVTVGVIGSGDFAKSLTIRLIRCGYHVVIGS 60
pdb|6HCY|C               MEKTCI---------DALPLTMN--SSEKQETVCIFGTGDFGRSLGLKMLQCGYSVVFGS 49
                         **. .:          ** :*  .. :: ** ::*;***.:** :::::*** **;:**

sp|Q8NFT2|STEA2_HUMAN    RNPKFASEFFPHVVDVTHHEDALTKTNIIFVAIHREHYTSLWDLRHLLVGKILIDVSNNM 120
pdb|6HCY|C               RNPQKT-TLLPSGAEVLSYSEAAKKSGIIIIAIHREHYDFLTELTEVLNGKILVDISNNL 108
                         ***: :   ::*   .:*   :.:*  .*:.**::****** *  :* .:* ****:*;:***;

sp|Q8NFT2|STEA2_HUMAN    RINQYPESNAEYLASLFPDSLIVKGFNVVSAWALQLGPKDASRQVYICSNNIQARQQVIE 180
pdb|6HCY|C               KINQYPESNAEYLAHLVPGAHVVKAFNTISAWALQSGALDASRQVFVCGNDSKAKQRVMD 168
                         :************* *_*.: ;**_**.**;****** *  *****::*_*; :*;:*;*;::

sp|Q8NFT2|STEA2_HUMAN    LARQLNFIPIDLGSLSSAREIENLPLRLFTLWRGPVVVAISLATFFFLYSFVRDVIHPYA 240
pdb|6HCY|C               IVRNLGLTPMDQGSIMAAKEIEKYPLQLFPMWRFPFYLSAVLCVFLFFYCVIRDVIYPYV 228
                         :.*:*.: *;* *** :*;:**: **;:*: :* *. :: *._*;:*.:.****;**.

sp|Q8NFT2|STEA2_HUMAN    RNQQSDFYKIPIEIVNKTLPIVAITLLSLVYLAGLLAAAYQLYYGTKYRRFPPWLETWLQ 300
pdb|6HCY|C               YEKKDNTFRMAISIPNRIFPITALTLLALVYLPGVIAAILQLYRGTKYRRFPDWLDHWML 288
                         :::.: ::: *.* *; ;**_*;***:****  *** ***_****** **; *;

sp|Q8NFT2|STEA2_HUMAN    CRKQLGLLSFFFAMVHVAYSLCLPMRRSERYLFLNMAYQQVHANIENSWNEEEVWRIEMY 360
pdb|6HCY|C               CRKQLGLVALGFAFLHVLYTLVIPIRYYVRWRLGNLTVTQAILKKENPFSTSSAWLSDSY 348
                         *******::; **;:** *;* :*;:*   *; : *;:;  :  : ** :; .;* : *

sp|Q8NFT2|STEA2_HUMAN    ISFGIMSLGLLSLLAVTSIPSVSNALNWREFSFIQSTLGYVALLISTFHVLIYGWKRAFE 420
pdb|6HCY|C               VALGILGFFLFVLLGITSLPSVSNAVNWREFRFVQSKLGYLTLILCTAHTLVYGGKRFLS 408
                         ::;:*;: *; **;:**;****** *;** ***;:;;_* *;**.*** ** ;:

sp|Q8NFT2|STEA2_HUMAN    EEYYRFYTPPNFVLALVLPSIVILGKIILFLPCISRKLKRIKKGWEKSQFLEEGMGGTIP 480
pdb|6HCY|C               PSNLRWYLPAAYVLGLIIPCTVLVIKFVLIMPCVDNTLTRIRQGWERNSKH--------- 459
                         .  ;*:* ;**.;;:*. *;; *;;:;:**;...*.**;:***;:.

sp|Q8NFT2|STEA2_HUMAN    HVSPERVTVM  490
pdb|6HCY|C               ----------  459
```

Figure 1: Sequence alignment of query sequence (metalloreductase STEAP2) and template sequence (6HCY)

Ala402, Ser406, His409, Val410, Asn431, Phe432, and Ala435.

Seventeen plant secondary metabolites were selected for molecular docking study. All the molecules were taken from NCBI PubChem compound database.[16] All the molecules were sketched in sybyl6.7[17] and minimized using Gasteiger-Huckel charges and by selecting Tripos force fields with distance-dependent electric function with 0.5 kcal/mol convergence criteria. Finally, the molecules were saved in .mol² format. AutoDock accepts .mol² or PDB files as input files. Molecular docking study was performed to all the ligands separately using AutoDock4.2[18] program, using the Lamarckian genetic algorithm and implemented empirical free energy function. Initially, the modeled metalloreductase STEAP2 protein was loaded and hydrogen was added and saved it in PDBQT format. Later, the ligand was loaded and set conformations and saved it in PDBQT format. The grid parameters were selected and calculated using autogrid. For all the dockings, a grid point spacing of 0.375 Å was applied and grid map with 60×60×60 points was used. Active site was predicted in sybyl6.7 biopolymer module. X, Y, and Z coordinates were selected on the basis of the amino acids present in the active site. Default parameters were used to run the AutoDock.

RESULTS AND DISCUSSION

Homology modeling and model evaluation

The present study reports that the query protein (Accession number: Q8NFT2) having high degree of homology with C chain of 6HCY protein was used as a template. The query sequence of Chain C, metalloreductase STEAP2 from *H. sapiens* having 490 amino acid residues was retrieved from the UniProt protein sequence database with Accession No. Q8NFT2. PDB Id 6HCY_C was identified and selected as template using BLAST having 47.50% identity and 68% positives. 3D model was generated using MODELLER 9.21 and the generated structure was validated using protein structure and by PROCHECK. The generated model showed 94.5% of amino acid residues (416 amino acids) in core region, 5.2% of amino acid residues (23 amino acids) in additionally allowed region, and 0.2% of the amino acid residues (1 amino acid) in the generously allowed region and there are no amino acids present in disallowed region.

Figure 2: Cartoon model of modeled metalloreductase STEAP2 protein

The template PDB shows 89.1% of amino acid residues (1035 amino acids) in core region, 10.2% of the amino acid residues (119) in additionally allowed region, and 0.6% of the amino acid residues (7 amino acids) in the generously allowed region and there are no amino acid residues in disallowed region. Cartoon model is shown in Figure 2 and Ramachandran plot of the modeled protein is shown in Figure 3. RMSD was calculated for template and generated model using SPDBV. Both the models were loaded and superimposed using carbon alpha and calculated RMSD. The superimposed model is shown in Figure
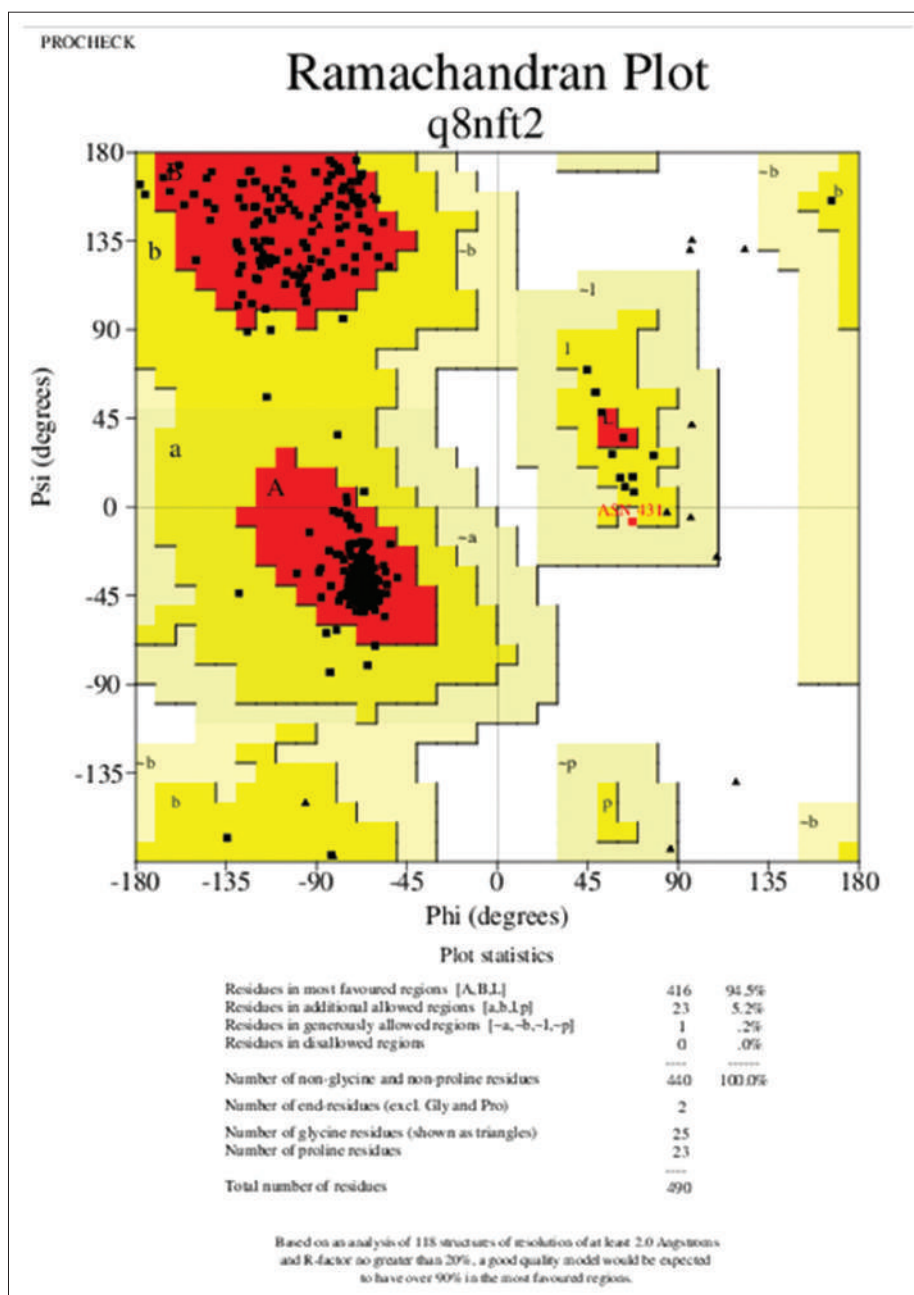
Figure 3: Ramachandran plot of the modeled metalloreductase STEAP2 protein

Table 1: Binding energies, interacting amino acid residues of all the 17 natural compounds and five already existing drugs as controls

C. No.	Compound name	Interacting amino acids	Binding energy ΔG (kcal/mol)	Dissociation constant (μM)
1	Artocarpin	Arg302, Tyr271	−7.21	5.22 μM
2	Artonin E	Lys303, Arg302, Leu299	−6.97	7.77 μM
3	Bartericin A	Gln300	−5.80	56.12 μM
4	Curcumin	Arg302, Lys303	−5.95	43.49 μM
5	Bilobetin	Ser392, Gln300	−7.49	3.24 μM
6	Erybraedin A	Lys303, Gln395	−7.95	1.49 μM
7	Daidzein	Arg302, Lys303, Gln395, Gln300	−6.32	23.32 μM
8	Biochanin	Thr210, Trp212, Ser378	−6.01	39.62 μM
9	Chaplashin	Arg302, Try271	−7.24	4.93 μM
10	Erystagallin A	Lys303, Arg302	−7.91	1.59 μM
11	Ginkgetin	Trp212, Thr210	−9.10	213.0 nM
12	Cudraflavone	Lys303	−7.42	3.62 μM
13	Luteolin	Gln395, Arg302, Tyr271, Gln300	−6.28	24.79 μM
14	Genistein	Lys303, Lys303, Arg302, Gln395	−6.32	23.26 μM
15	Hesperetin	Lys303, Arg302, Tyr271, Lys303	−6.30	23.99 μM
16	Medicagenin	Lys303, Arg302	−7.95	1.48 μM
17	Isoginkgetin	Lys303, Tyr271	−7.53	3.01 μM
18	Mitoxantrone*	Ser392	−1.99	34.63 mM
19	Abiraterone acetate*	Tyr271	−7.19	53.6 μM
20	Apalutamide*	Gln304, Ser363	−6.26	25.79 μM
21	Enzalutamide*	Gln304, Ser383	−5.90	47.02 μM
22	Flutamide*	Gln395	−6.21	28.24 μM

*Indicates existing drugs
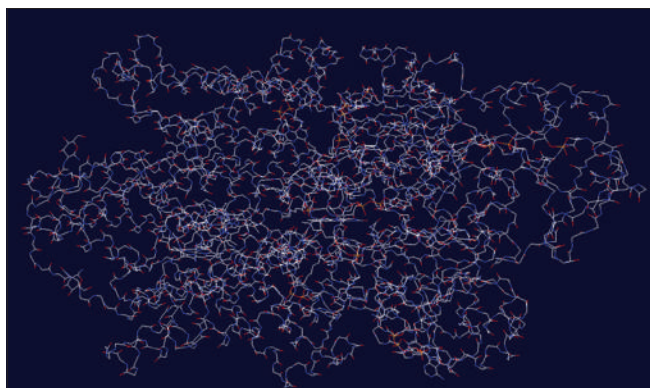
Figure 4: Superimposed model of modeled metalloreductase STEAP2 (query) and 6HCY (template)

4. It showed RMSD of 1.62 Å, which indicates the generated model shows similar function as template.

Molecular docking results

Molecular docking is the most extensively used method for the calculation of protein-ligand interactions. In the present study, the native plant secondary metabolites (flavonoid molecules) have been identified as metalloreductase STEAP2 protein inhibitors. AutoDock4.2 uses binding free energy assessment to assign the best binding conformation. Seventeen potent molecules were allowed individually for docking and also used five already existing drugs as standards for docking study against modeled protein. Docking study has shown the H-bonding of Ginkgetin with Trp212 and Thr210 residues of modeled protein with a docking score value of −9.10 kcal/mol. Compound medicagenin exhibited binding energy of −7.95 kcal/mol with interacting Lys303 and Arg302. Twelve compounds exhibited binding energy values ranging from −6.01 to −7.00 Kcal/mol. Two compounds erybraedin A and medicagenin exhibited same binding energies of −7.95 kcal/mol with Lys303, Gln395 and Lys303, Arg302, respectively. All the compounds binding energies and interacting amino acids are shown in Table 1. Table 1 numbers match with Figure 5 numbers.
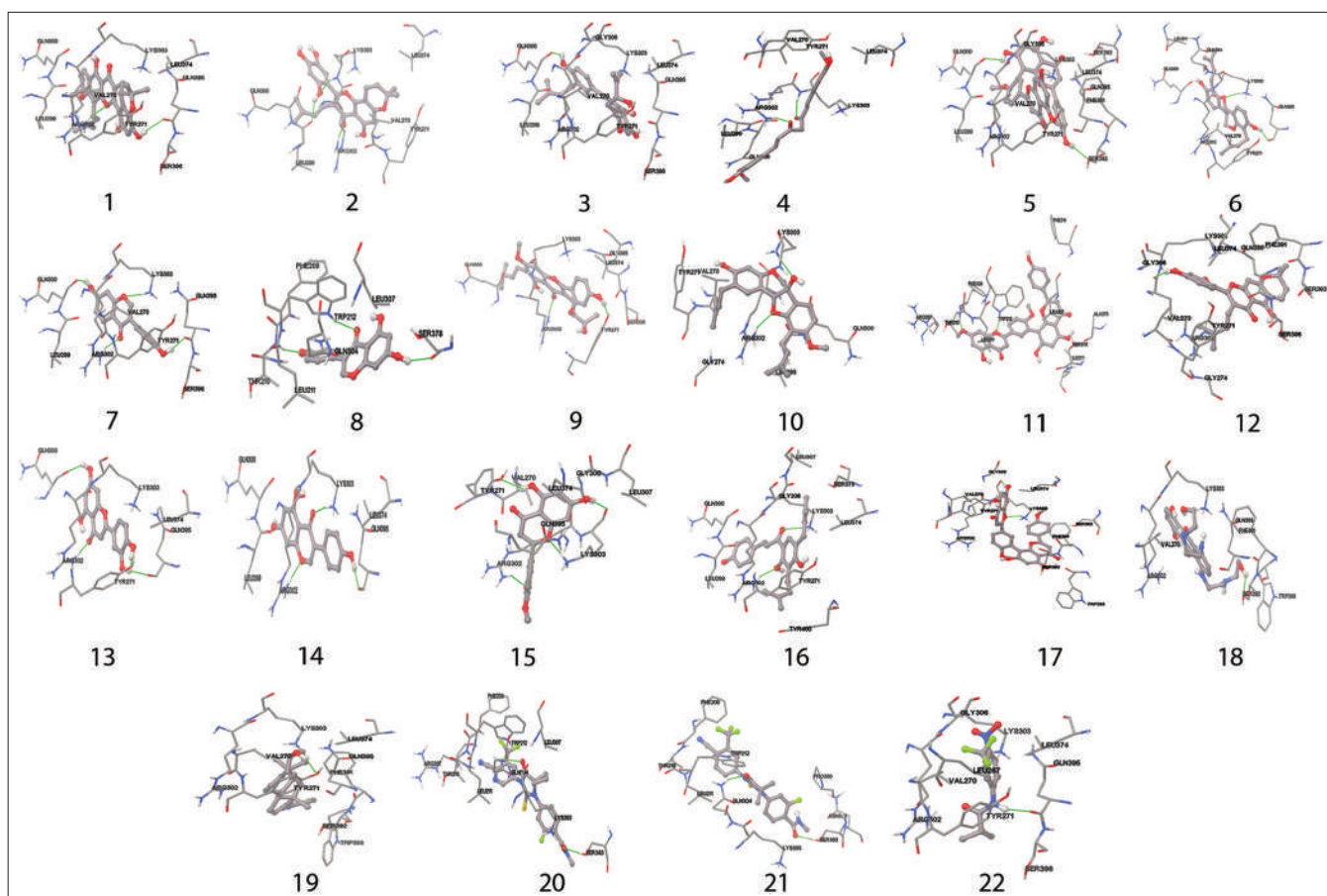
Figure 5: Docking of 17 natural compounds and standard drugs against modeled metalloreductase STEAP2 protein

CONCLUSION

The 3D model of the metalloreductase STEAP2 from *H. sapiens* was developed using molecular modeling method. Human STEAP4 bound to nicotinamide adenine dinucleotide phosphate, flavin adenine dinucleotide, heme, and Fe (III)-NTA (PDB ID: 6HCY_C) was used as template to predict the model. The predicted model showed 94.5% of amino acid residues in the most favored region. Active site amino acid residues of the metalloreductase STEAP2 model have been identified. Molecular docking studies were also performed to the modeled protein by taking 17 natural flavonoid compounds. All the compounds exhibited lowest binding energies and interactions than already existing drugs, which may lead to potent inhibitors for metalloreductase STEAP2.

REFERENCES

1. Whiteland H, Spencer-Harty S, Morgan C, Kynaston H, Thomas DH, Bose P, *et al.* A role for STEAP2 in prostate cancer progression. Clin Exp Metastasis 2014;31:909-20.
2. Wright JL, Lange PH. Newer potential biomarkers in prostate cancer. Rev Urol 2007;9:207-13.
3. D'Amico AV, Whittington R, Malkowicz SB, Schultz D, Blank K, Broderick GA, *et al.* Biochemical outcome after radical prostatectomy, external beam radiation therapy, or interstitial radiation therapy for clinically localized prostate cancer. JAMA 1998;280:969-74.
4. Duffy MJ, McGowan PM, Gallagher WM. Cancer invasion and metastasis: Changing views. J Pathol 2008;214:283-93.
5. Gunshin H, Mackenzie B, Berger UV, Gunshin Y, Romero MF, Boron WF, *et al.* Cloning and characterization of a mammalian proton-coupled metal-ion transporter. Nature 1997;388:482-8.
6. Fleming MD, Romano MA, Su MA, Garrick LM, Garrick MD, Andrews NC, *et al.* Nramp2 is mutated in the anemic Belgrade (b) rat: Evidence of a role for nramp2 in endosomal iron transport. Proc Natl Acad Sci U S A 1998;95:1148-53.
7. Ohgami RS, Campagna DR, McDonald A, Fleming MD. The steap proteins are metalloreductases. Blood 2006;108:1388-94.
8. Wang L, Jin Y, Arnoldussen YJ, Jonson I, Qu S, Maelandsmo GM, *et al.* STAMP1 is both a proliferative and an antiapoptotic factor in prostate cancer. Cancer

Res 2010;70:5818-28.

9. Hasegawa H, Li C, Alba BM, Penny DM, Xia Z, Dayao MR, *et al.* Membrane cholesterol modulates STEAP2 conformation during dynamic intracellular trafficking processes leading to broad subcellular distribution. Exp Cell Res 2018;370:208-26.

10. Available from: https://www.uniprot.org/uniprot/Q8NFT2. Last modified: June 5, 2019

11. Altschul SF, Gish W, Miller W, Myers EW, Lipman DJ. Basic local alignment search tool. J Mol Biol 1990;215:403-10.

12. Oosterheert W, van Bezouwen LS, Rodenburg RNP, Granneman J, Förster F, Mattevi A, *et al.* Cryo-EM structures of human STEAP4 reveal mechanism of iron (III) reduction. Nat Commun 2018;9:4337.

13. Laskowski RA, MacArthur MW, Moss DS, Thornton JM. PROCHECK a program to check the stereochemical quality of protein structures. J Appl Crystallogr 1993;26:283-91.

14. Larkin MA, Blackshields G, Brown NP, Chenna R, McGettigan PA, McWilliam H, Valentin F, Wallace IM, Wilm A, Lopez R, Thompson JD, Gibson TJ, Higgins DG. Clustal W and Clustal X version 2.0. Bioinformatics. 2007;23:2947-2948.

15. Webb B, Sali A. Comparative Protein Structure Modeling Using Modeller. Current Protocols in Bioinformatics. Vol. 54. Hoboken, NJ, USA: John Wiley and Sons 2016; p. 5.6.1-5.6.37.

16. https://www.ncbi.nlm.nih.gov/pccompound

17. Tripos Sybyl 6.7, Inc. St. Louis, Missouri 63144, USA.

18. Morris GM, Huey R, Lindstrom W, Sanner MF, Belew RK, Goodsell DS, *et al.* AutoDock4 and autoDockTools4: Automated docking with selective receptor flexibility. J Comput Chem 2009;30:2785-91.